Journal of Catalysis **188,** 69–82 (1999)
Article ID jcat.1999.2653, available online at http://www.idealibrary.com on IDEAL®

A Steady-State Isotopic Transient Kinetic Analysis of the $NO/O_2/H_2$ Reaction over Pt/SiO_2 Catalysts

R. Burch, A. A. Shestov,[1] and J. A. Sullivan

Catalysis Research Centre, Chemistry Department, University of Reading, Whiteknights, Berks, RG6 6AD, United Kingdom

Received February 24, 1999; revised May 21, 1999; accepted August 2, 1999

The $NO/O_2/H_2$ reaction under strongly oxidising conditions has been studied over a 5% Pt/SiO_2 catalyst using Steady-State Isotopic Transient Kinetic Analysis (SSITKA). The ^{14}N-containing reactants and products were monitored following a $^{14}NO/O_2/H_2 \rightarrow {}^{15}NO/O_2/H_2$ switch. N_2O was found to be the isotopically first product and N_2 the isotopically second. It was found that there was a constant desorption of NO from the catalyst surface under steady-state conditions. Recently introduced transformations (IDIMP, TRIMP, and the semilogarithmic plot of the $\bar{\alpha}$ function versus time) of the product profiles, which concentrate on the isotopic distribution of the product molecules following the $^{14}NO \rightarrow {}^{15}NO$ switch, are used to analyse the mechanism of N_2 formation from this reaction. These show that N_2 formation is predominantly through an "impact" route in which gaseous or physisorbed NO reacts with a reduced N species on the catalyst in a modified Eley–Rideal mechanism. A second, less active, mode of N_2 formation is through the interaction of two equivalent species on the surface, each of which gives one N atom to the N_2 molecule. The presence of O_2 results in a change in the relative contribution of each type of N_2 production.

Key Words: **NO*x* reduction; H_2 reductants; lean burn; SSITKA.**

INTRODUCTION

NO*x* removal using hydrocarbon reductants in an oxidising environment has attracted recent attention (1, 2) for after-treatment systems for diesel and lean-burn gasoline engines (3, 4). Pt catalysts seem most promising (5, 6), and various reductants (CH_4, C_2H_4, C_3H_6, C_3H_8, C_8H_{18}) (7, 8) have been studied. It has been found that the reaction mechanism and hence the activity for the deNO*x* reaction is strongly dependent on the choice of reductant.

H_2 is not, in general, a selective reductant since it reacts preferentially with O_2 rather than with NO*x* (9). However, it has recently been found that the reduction of NO*x* in an oxidising environment can be performed with H_2 on Pt catalysts at low temperatures. The formation of N_2O remains a problem, however, and it is found that at low temperatures the selectivity to N_2O can be over 50% (10–13).

SSITKA is a valuable technique (14, 15) which can be used for the determination of the number and activity of catalytic sites on a catalyst under *actual* reaction conditions (16–18). It has been used, for example, to study the Fischer–Tropsch reaction (19) and the selective reduction of NO using CH_4 (20). Generally, the reactions from which most information is gained are those in which there are large reservoirs of relatively inert surface intermediates which form product molecules.

We have previously used the SSITKA technique to study the $NO/C_3H_6/O_2$ (21) and the NO/H_2 (11) reactions over supported Pt catalysts and, using mathematical modelling techniques, have developed several criteria for the analysis of the product profiles in order to obtain information about the nature of surface intermediates, and thus an improved understanding of the reaction mechanism (11).

Since the development of the SSITKA technique there have been numerous papers devoted to the numerical analysis of SSITKA profiles with the aim of generating information about reaction mechanisms. These numerical analyses have generally taken the form of modelling the transient data generated from either continuously stirred tank (22, 23) or plug flow (24) reactors. Comprehensive reviews of the technique have been published (14, 15). However, it is generally the case that most workers have analysed isotope transfer only, i.e., the fraction of isotopes within the reactant and product components with time. Distribution of isotopic molecules has been disregarded or only partially considered without detailed qualitative analysis of experimental data (25).

In this paper we describe several methods of analysing the data obtained from isotopic transients in order to try to develop information about the reaction mechanism. Some features of these methods originally come from classical isotopic exchange analysis in closed systems without the occurrence of chemical changes in the system (26–33). We have extended these analyses to SSITKA studies for use in a flow system with the occurrence of chemical change.

[1] On leave from Boreskov Institute of Catalysis, Russian Academy of Sciences, Pr. Akademika Lavrentieva, 5, Novosibirsk, 630090, Russia.

0021-9517/99 $30.00

Specifically, our approach will be for situations where a reactant molecule (RA_n) containing labelled atoms (where there are two possible isotopes for the A element) is converted, via intermediates (IA_x), into a product molecule that contains two such labelled atoms (PA_2) for a steady-state reaction in a plug flow reactor, e.g., $^*NO + H_2 \rightarrow {}^*N_2/{}^*N_2O$, where $*$ represents a labelled atom. A full mathematical description of the methodology used in the interpretation and modelling of these results is presented elsewhere (34). Only the essential details are given here.

EXPERIMENTAL

The catalytic system used in this study has been described fully elsewhere (21). The catalyst is 5% Pt/SiO_2 prepared by incipient wetness from a Pt(DNDA) solution. The surface area of the catalyst was $\sim$260 $m^2\ g^{-1}$ and the metal dispersion was 31%, corresponding to an exposed metal surface of 4.74×10^{19} atoms g^{-1} (3.78 $m^2\ g^{-1}$). These values were measured using an "in-house" BET and H_2-chemisorption apparatus. One hundred and thirteen milligrams of the catalyst was placed in a quartz reactor tube, preceded by 100 mg of quartz chips which preheated the incoming gas (particle size, 250–850 μm; reactor diameter, 4 mm). The reaction mixture was 1.64% NO, 1.64% H_2, 8.7% O_2, in an He carrier gas at a total flow of 113 $cm^3\ min^{-1}$.

The temperature programmed reaction was carried out after the catalyst was pretreated in the reaction mixture for 1 h at 400°C and the catalyst was cooled in the reaction mixture and ramped in He to 500°C at a rate of 5°C min^{-1}. The effluent was continuously monitored for NO, NO_2, N_2, N_2O, H_2O, and NH_3, as the temperature was ramped, using a "Gaslab" mass spectrometer. The absolute amounts of desorbed products were calculated using calibration plots of mass spectrometer responses against partial pressure.

The SSITKA switches involved taking a catalyst to a steady state in $^{14}NO/O_2/H_2$ and then switching out the ^{14}NO and replacing it with an equivalent flow (and pressure) of ^{15}NO. The original flow of ^{14}NO also contained a 5% Ar tracer, the decay in which was used to monitor the gas-phase holdup of the system ($\sim$1.5 s). Differences between the pressures of the lines arise from the fact that the gas that is being used as a reactant is flowing through the catalyst and thus experiences some back-pressure. The pressure in the ^{14}NO and ^{15}NO lines are measured using two "Wika" pressure transducers and are equalised using a fine needle valve.

Following this switch, the reactor effluent is continuously monitored for all isotopic molecules of NO (at $m/e = 30$ and 31), N_2 (at 28 and 29), NO_2 (at 46 and 47), and N_2O (at 44 and 45). Overlaps in the $m/e = 30$ and $m/e = 46$ peaks (where ^{14}NO and $^{15}N_2$ and $^{15}N_2O$ and $^{14}NO_2$ share m/e values) are allowed for by considering that the overall production of N_2 and N_2O are not changed by the switch from ^{14}NO to ^{15}NO. Thus the relevant profiles for $^{15}N_2$ and $^{15}N_2O$ can be mathematically generated using the fact that the normalised production of N_2 and N_2O at any time following the switch must equal 1. In a similar manner the profile for the upcoming $^{15}NO_2$ species following the $^{14}NO \rightarrow {}^{15}NO$ switch is used to calculate the expected decrease in the $^{14}NO_2$ signal.

The use of the reverse switch, i.e., $^{15}NO \rightarrow {}^{14}NO$, after a prolonged period in the $^{15}NO/O_2/H_2$ reaction mixture allows the measurement of upcoming $^{14}N_2$ and $^{14}N_2O$ profiles, which are what would be expected for the $^{15}N_2$ and $^{15}N_2O$ profiles from the original $^{14}NO \rightarrow {}^{15}NO$ switch. These profiles are approximately the same as those mathematically generated by the above-mentioned process.

For the TRIMP, IDIMP, and semilogarithmic analyses (see below) the experiment was modified in order to further minimise the pressure change. This was achieved by reducing the overall flow rate to 73 $cm^3\ min^{-1}$, leading to a gas composition of 2.5% NO, 2.5% H_2, 14.8% O_2 in an He flow. This experiment was performed at 70°C.

RESULTS

Temperature Programmed Reaction

Figure 1 shows the production of N_2, N_2O, and NO_2 as a function of temperature. This profile is in qualitative agreement with that measured under steady-state conditions (10). The production of N_2O peaks at $\sim$100°C while the N_2 reaches a broad maximum between $\sim$110 and 140°C. The production of NO_2 is seen at temperatures lower and higher than the maxima in the N_2O and N_2 profiles. The

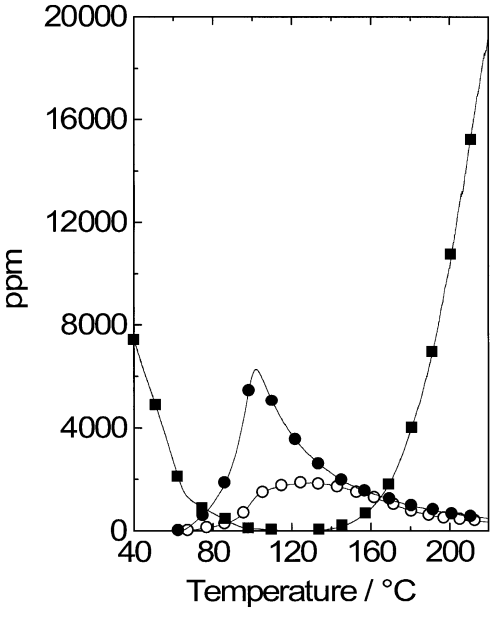

FIG. 1. Temperature programmed reaction of $NO/H_2/O_2$ over a 5% Pt/SiO_2 catalyst. The reactant stream contained 1.64% NO, 1.64% H_2, and 8.7% O_2 with an He carrier gas in a total flow of 113 $cm^3\ min^{-1}$ and catalyst mass = 113 mg: N_2 (○), N_2O (●), and NO_2 (■).

lower temperature formation of NO_2 is due to the gas-phase interaction of NO molecules with O_2 molecules. The higher temperature production of NO_2 is ascribed to the interaction of $NO_{(g)}$ with O_{ads} on the catalyst surface.

The trend in selectivity for the N_2 and N_2O products is the same as that observed previously for the NO/H_2 reaction (11). The catalyst is far more selective to N_2O than to N_2 at these temperatures. In contrast to the NO/H_2 reaction no NH_3 is formed. This is reasonable because the gas phase is oxidising and NH_3 would only be expected to be formed under reducing conditions.

Steady-State Isotopic Transient Kinetic Analysis

Two temperatures (60 and 83°C), where the conversion of NO was quite low, were chosen for the SSITKA of the $NO/O_2/H_2$ reaction over the 5% Pt/SiO_2 catalyst. The rates of production of N_2 and N_2O, as well as the flow rate of unreacted NO under these conditions, as a function of the temperature of reaction, are presented in Table 1. The rates of reaction are calculated from the total observed change in $^{14}N_2$ (or $^{14}N_2O$) signal upon removal of the ^{14}NO and insertion of the ^{15}NO.

It can be seen (Table 1) that the rates of production of N_2 and N_2O increase as the temperature is raised. Figure 2 shows the normalised isotopic product responses following the $^{14}NO/H_2/O_2 \rightarrow {}^{15}NO/H_2/O_2$ switch over the 5% Pt/SiO_2 catalyst at $T = 83$°C. Plots relating to the Ar (and its inverse) signal are also shown for reference.

The product plots have much in common with profiles observed earlier for the $C_3H_6/NO/O_2$ (21) and NO/H_2 (11) systems. The decrease in production of unlabelled N_2 (△) and N_2O (▲) is instantaneous with the switch, as is the production of mixed-labelled N_2 (○) and N_2O (●). The mixed-labelled N_2 and N_2O profiles rise through maxima very shortly after the switch and begin to decrease after this time. A mathematically generated $^{15}N_2$ profile (◇) is also seen to increase from zero shortly after the switch, as is the generated $^{15}N_2O$ profile (◆).

TABLE 1

Rates of Formation of N_2 and N_2O and the Flow Rate of Unreacted NO (μmol g^{-1} s^{-1}) over a 5% Pt/SiO_2 Catalyst at Two Temperatures in an $NO/O_2/H_2$ Stream

T°C	$r(N_2)$	$\tau(N_2)$	$r(N_2O)$	$\tau(N_2O)$	$r(NO)$	$\tau(NO)$
60	0.04	64 ± 0.5	0.46	1.1 ± 0.5	10.01	0.6 ± 0.5
83	0.09	42 ± 0.5	1.27	0.7 ± 0.5	8.53	0.8 ± 0.5

Note. Also shown are values for τ (the mean surface residence time (s)) for the products and reactant as determined from SSITK analysis. The reactant stream contained 1.64% NO, 1.64% H_2, and 8.7% O_2 with an He carrier gas in a total flow of 113 cm^3 min^{-1} over a 5% Pt/SiO_2 catalyst (113 mg).

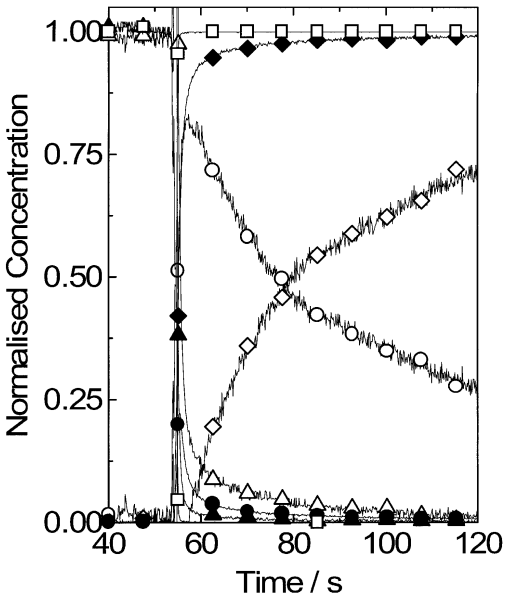

FIG. 2. Normalised product responses following the replacement of $^{14}NO/Ar$ with ^{15}NO in the reaction stream. Reaction conditions: 1.64% NO, 1.64% H_2, and 8.7% O_2 with an He carrier gas in a total flow of 113 cm^3 min^{-1}, catalyst mass = 113 mg, $T = 83$°C. $^{14}N_2$ (△), $^{14}N^{15}N$ (○), $^{15}N_2$ (◇), $^{14}N_2O$ (▲), $^{14}N^{15}NO$ (or $^{15}N^{14}NO$) (●), $^{15}N_2O$ (◆), Ar and Inverse Ar (□).

It is seen that the unlabelled N_2O signal reaches a value of zero more rapidly than that of the unlabelled N_2 species. The same is true of the profile relating to the mixed-labelled N_2O relative to the mixed-labelled N_2 profile. This is more clearly seen in Fig. 3, where the α profiles for N_2 (■) and N_2O (●) are presented along with the profile for ^{15}NO (○) and $^{15}NO_2$

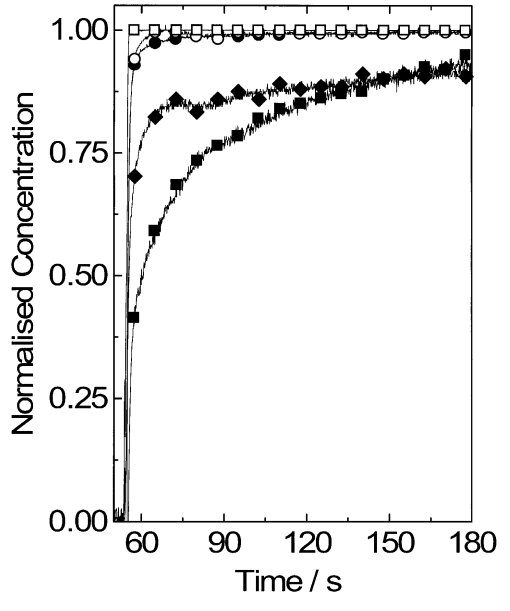

FIG. 3. The α N_2 (■), αN_2O (●), ^{15}NO (○), $^{15}NO_2$ (◆), and inverted Ar (□) profiles from the experiment shown in Fig. 2.

(◆). The α function has previously been described as the fraction of reactant or product that is made up of labelled (^{15}N) atoms following the $^{14}NO \rightarrow {}^{15}NO$ switch (21); i.e., in the case of N_2, $\alpha(N_2)$ is defined as

$$\alpha(N_2) = \frac{[^{15}N_2] + 0.5[^{15}N^{14}N]}{[^{15}N_2] + [^{14}N^{15}N] + [^{14}N_2]}. \quad [1]$$

A similar function can be constructed for $\alpha(N_2O)$ while $\alpha(NO)$ and $\alpha(NO_2)$ can be taken directly from the normalised ^{15}NO and $^{15}NO_2$ readings. It is seen that the $\alpha(N_2O)$ and $\alpha(NO)$ plots are, to a first approximation, the same as one another. This is a situation that has been seen before for the NO/H_2 system (11) and shows that N_2O which contains an ^{14}N atom can only continue to be formed for as long as there is ^{14}NO in the system.

In contrast to this, when the $NO/C_3H_6/O_2$ system (21) was studied over the same catalysts, below the temperature of hydrocarbon "light-off" it was found that there was no difference between the Ar profile and that of the ^{15}NO. This indicated that there was no steady-state desorption of NO from the catalyst while it was operating in the case of the $NO/C_3H_6/O_2$ reaction (below hydrocarbon "light-off") but that such a desorption does take place in the case of the NO/H_2 and $NO/H_2/O_2$ reactions.

The $\alpha(N_2)$ and $\alpha(NO_2)$ profiles are very far removed from the Ar profile and are delayed for ~250 s before reaching a normalised value of 1. In the case of the N_2 product this is a situation that was also seen in the case of the NO/H_2 reaction (11) and also the $NO/C_3H_6/O_2$ reaction (21); i.e., N_2O, was the isotopically first product and N_2 was the isotopically second.

In the case of NO_2 the situation is a little more complex. There was a delay in the removal of NO_2 from the reactor following the $^{14}NO \rightarrow {}^{15}NO$ switch, and this delay was not associated with the catalyst as it was also present when quartz chips were used alone in the reactor *and* when the reactor was empty. The production of NO_2 was rather small and *decreased* as the temperature was raised from 60 to 83°C, and thus the normalised plots of $^{15}NO_2$ became very noisy (as the difference between normalised values of 0 and 1 are small). However, the order of the labelled molecules in the effluent always remained $NO \approx N_2O$, followed by NO_2 followed by N_2.

From a standard SSITKA (14) the difference in area between the Ar profile and the various α profiles can be used to obtain a value for the mean surface residence time (τ) for the species on the surface leading to products. For example, in the case of N_2,

$$\tau(N_2) = \int_0^\infty \bar{\alpha}(N_2)\, dt, \quad [2]$$

where $\bar{\alpha}$ represents the $(1-\alpha)$ profile in the case of the ^{14}NO to ^{15}NO switch and the α profile in the case of the ^{15}NO to ^{14}NO switch. The "mean surface residence times" (τ) of the species leading to products, as well as the rates of formation of the various products, are shown as a function of temperature in Table 1. It can be seen that the increase in temperature between 60 and 83°C resulted in a decrease in the mean surface residence times for N_2 and N_2O.

These values (τ and r) can be used to yield values for the concentration of adsorbed surface species leading to product and of adsorbed reactant which simply desorbs. For example, in the case of N_2 or N_2O this is calculated from the relationship

$$2 * \tau_{(N_2 \text{ or } N_2O)} * r_{(N_2 \text{ or } N_2O)} = N_{(N_2 \text{ or } N_2O)}, \quad [3]$$

where τ is the mean surface residence time (s), r is the rate of production of the product molecule (μmol g^{-1} s^{-1}), and N is the concentration of active sites (μmol g^{-1}). The number 2 represents the number of atoms of labelled element per molecule (2 in the case of N_2 and N_2O, 1 in the case of NO and NO_2). A more general method for calculating the surface concentrations of adsorbed intermediates using the α functions has been proposed previously (21).

Table 2 shows the calculated concentration of sites on the surface as determined from this analysis at the two temperatures studied. It can be seen that the reason for the increase in the activity of the catalyst for the production of N_2 is due to an increase in the concentration of sites (5.1 → 7.6 μmol g^{-1}) active for the production of N_2 and to an increase in the overall "reactivity" of these sites (as qualitatively measured by the reciprocal of the mean surface residence time, which decreases from 64 to 42 s). It should be remembered that this is a qualitative measurement only and only truly holds for unidirectional first-order reactions.

The increase in the production of N_2O is *more* due to an increase in the concentration of sites (1 → 1.8 μmol g^{-1}) active for its production although the "activity" of the sites also increases somewhat (1.1 → 0.7 s). The determination of the increase in the activity and concentrations of the sites that produce N_2O is heavily influenced by errors in the calculation of τ (estimated as 0.5) while such errors are less influential in the case of the production of N_2—as its residence time is considerably higher.

TABLE 2

Concentrations of Adsorbed Species N (μmol g^{-1}) on the Surface of 5% Pt/SiO_2 as a Function of Temperature during the $NO/H_2/O_2$ Reaction as Measured by SSITK Analysis

	$N(N_2)$	$N(N_2O)$	$N(NO)$	$\sum N$
60	5.1 ± 0.04	1.0 ± 0.5	6.0 ± 5	12.1 ± 5.5
83	7.6 ± 0.1	1.8 ± 1.3	6.8 ± 4.3	16.2 ± 5.7

Note. The reactant stream contained 1.64% NO, 1.64% H_2, and 8.7% O_2 with an He carrier gas in a total flow of 113 cm^3 min^{-1} over a 5% Pt/SiO_2 catalyst (0.113 g).

TABLE 3

Coverages of Surface Intermediates Θ (×100) on 5% Pt/SiO_2 as a Function of Temperature during the $NO/H_2/O_2$ Reaction as Measured by SSITK Analysis

	$\Theta(N_2)$	$\Theta(N_2O)$	$\Theta(NO)$	Θ
60	6 ± 0.1	1 ± 0.6	8 ± 6.4	16 ± 7.1
83	10 ± 0.1	2 ± 1.6	9 ± 5.4	20 ± 7.1

Note. The reactant stream contained 1.64% NO, 1.64% H_2, and 8.7% O_2 with an He carrier gas in a total flow of 113 $cm^3\,min^{-1}$ over a 5% Pt/SiO_2 catalyst (0.113 g). The Pt catalyst had 4.74×10^{19} Pt atoms exposed to the gas phase.

The concentration of adsorbed species can be related to the metal surface area of the Pt. Table 3 shows the metal surface coverage of species leading to N_2 and N_2O as well as the surface coverage of adsorbed unreacted NO as a function of temperature during the $NO/H_2/O_2$ reaction. It is seen that the calculated surface coverages of N_2 and N_2O precursors on the surface are 6 and 1%, respectively, at 60°C, and these values increase to ∼10 and ∼2%, respectively, as the temperature is raised to 83°C. Note again that the errors in the calculation of the $\tau(N_2O)$ value result in substantial errors in the calculation of the $N(N_2O)$ value and thus in the $\Theta(N_2O)$ value. However, even taking these substantial errors into account the surface coverage of intermediates which go on to form N_2O is far lower than that of intermediates which go on to form N_2.

The coverages of unreacting NO, which is also heavily influenced by possible error in the calculation of $\tau(NO)$, remains rather constant between the two temperatures. The overall surface coverage of NO-derived species increases from ∼16 to ∼20%, showing that the surface of the Pt is never fully covered with N-containing species that either desorb or go on to form products. Even at the upper limit of the possible NO-derived surface coverage (∼27%) most of the Pt sites are not covered with species that (a) form N_2, (b) form N_2O, or (c) desorb as unreacted NO.

The remainder of the surface could be covered with H_2- or O_2-derived species or covered by NO-derived spectator species that are stable under these conditions. It is known (35) from TPD experiments that $NO_{2,ads}$-type species can form on Pt and that these species are relatively stable at the temperatures used here.

DISCUSSION

There are similarities between the results presented here and those seen before in the analysis of the $NO/C_3H_6/O_2$ (21) and NO/H_2 (11) reactions. On a quantitative level it is again seen that the reason for the increase in the production of N_2 with temperature is due to an increase in the concentration and activity of sites which produce N_2. The increase in production of N_2O with temperature is *more* due to an increase in the concentration of sites which produce N_2O than to an increase in their activity. The production of N_2O requires the presence of some reversibly adsorbed NO molecules to proceed. The isotopic order of production of the product molecules (N_2 and N_2O), following the switch, is again the same, with N_2O being isotopically first and N_2 being isotopically last. This leads to the exclusion of several mechanisms and must lead to the development of a mechanism in which N_2O is produced from earlier intermediates in a reaction sequence than those that produce N_2 (21).

In order to provide a more detailed mechanism for the reaction, we shall use three different analyses (and transformations) of the experimental profiles for the $NO + H_2$ reaction in relation to the information they yield about the N_2 and N_2O forming reactions. These analyses are: (a) the Initial Distribution of Isotopic Molecules of Product (IDIMP), which gives some information about the possibilities of there being more than one route to the formation of various products; (b) the Temporal Redistribution of the Isotopic Molecules of Product, (TRIMP), which gives information about the nature of the final intermediates on the surface before the final act of production of the doubly labelled product molecule; and (c) a semilogarithmic plot of the $\bar{\alpha}$ function versus time (where α is the fraction of heavy atoms in the gas phase), which tells of the presence of buffer states, consecutive, parallel routes, etc.

IDIMP is a "snapshot" of the initial redistribution immediately following a $^{14}NO + H_2 \rightarrow {}^{15}NO + H_2$ switch, while TRIMP and the semilogarithmic plot are presented as functions of time. It should be noted that IDIMP has been used previously for studying reactions such as benzene hydrogenation in flow systems (36, 37). The TRIMP plots relate to isotopic equilibrium, a concept which has been previously studied in isotopic exchange reactions (see below), although never in terms of SSITKA. The first two sets of profiles, (a) and (b), are discussed in terms of the concept of "Types of Production" of two-atom labelled molecules (PA_2). The IDIMP plots are also used to introduce the concept of the integral characteristics of any network mechanism of the form $RA_n \rightarrow \ldots IA_x \ldots \rightarrow PA_2$, i.e., where a labelled reactant (RA_n) progresses through one or more surface intermediates (IA_x) to yield a two-atom labelled molecule (PA_2). Full details can be found elsewhere (34), but the main features of these analyses are described below.

TYPES OF PRODUCTION OF TWO-ATOM LABELLED MOLECULES

In order to discuss the first and second transformations (IDIMP and TRIMP) of the data we introduce the concept of "Types of Production." This involves discriminating between alternative steady-state reaction mechanisms on the basis of the *final* reaction step leading to the generation

TABLE 4

The Five Possible Types of Production of a Product Molecule PA_2 from a Reactant Molecule RA and Reaction Intermediates (IA and I′A) and the Final Reaction Steps

Type of production	Mechanism of final step	Temporal redistribution $y_i = x_i - x_i^{eq}$	Initial distribution $\{x_0^0, x_1^0, x_2^0\}$	Production coefficient C_{PR}	Percolation coefficient C_{PE}
0	$2RA \rightarrow PA_2$	$y_1 = y_2 = 0$	{0, 0, 1}	0	2
1	$RA + IA \rightarrow PA_2$	$y_1 > 0, y_2 < 0$	{0, 1, 0}	1	1
2a	$2IA \rightarrow PA_2$	$y_1 = y_2 = 0$	{1, 0, 0}	2	0
2b	$IA + I'A \rightarrow PA_2$	$y_1 > 0, y_2 < 0$	{1, 0, 0}	2	0
2c	$IA_2 \rightarrow PA_2$	$y_1 < 0, y_2 > 0$	{1, 0, 0}	2	0

Note. Also shown are the predicted deviations of the fraction of isotopic molecules ($PA_{2-i}{}^*A_i$) from equilibrium (x_i^{eq}) of the isotopically labelled molecules (y_1 P^*AA and y_2 PA^*A^*), the expected initial isotopic distribution following the same switch, and the expected production (C_{PR}) and percolation (C_{PE}) coefficients following a step change $RA \rightarrow RA^*$.

of the product molecule (PA_2) from the reactant (RA_n) and any final intermediates on the surface (IA_x or $I'A_x$).

Detailed analysis (34) of the modes of production of a molecule of product (PA_2) containing two "labellable" A atoms from a labelled reactant molecule (RA_n) and intermediates IA_x has shown that there are basically five "pure" Types of Production of such molecules. These are shown in Table 4 and are briefly discussed below. In the following presentation, "A" represents a labelled atom (with two possible isotopes), RA_n represents a reactant containing "n" such atoms, PA_2 represents a product containing two such A atoms, and IA_x represents an intermediate containing "x" A atoms. R, P, and I are parts of the molecule that do not contain any A atoms (or contain A atoms that remain unreactive). We will consider a singly labelled reactant (RA) and either singly or doubly labelled intermediates, i.e., $x = 1$ or 2 (IA and IA_2), to simplify the types of production that we will discuss.

The first type of production (labelled 0) is one in which the surface plays no measurable role and the production of PA_2 involves no surface A atoms, i.e.,

$$\text{Type 0} \quad 2RA \rightarrow PA_2. \qquad [4]$$

The second type (labelled 1) involves, for example, an impact mechanism in which a molecule of RA interacts with a surface intermediate. Each of these species yields one A atom to produce a PA_2 molecule. This involves one surface A atom in the elementary act of production of PA_2, i.e.,

$$\text{Type 1} \quad RA + IA \rightarrow PA_2. \qquad [5]$$

The third, fourth, and fifth methods of formation of PA_2 all involve two surface A atoms in the final act of production. This these are labelled "2" and are differentiated on the basis of different types of final interactions. Production type 2a (a for alone) represents the formation of a PA_2 molecule from two equivalent moieties on the surface, both of which give one A atom to the final product, i.e.,

$$\text{Type 2a} \quad 2IA \rightarrow PA_2. \qquad [6]$$

Production type 2b (b for binary) represents the formation of PA_2 from the interaction of two *different* surface species, both of which give 1 A atom to the final product, i.e.,

$$\text{Type 2b} \quad IA + I'A \rightarrow PA_2. \qquad [7]$$

The final type of production of PA_2 is type 2c (c for coupled), and this involves the presence of a "coupled" intermediate on the surface which contains, as a minimum, two A atoms. In this case both atoms that go on to form PA_2 originate from the same species, i.e.,

$$\text{Type 2c} \quad IA_2 \rightarrow PA_2. \qquad [8]$$

These different types of production lead to different responses in the first and second features of the obtained profiles, i.e., Initial Distribution of Isotopic Molecules of Product (IDIMP) and Temporal Redistribution of Isotopic Molecules of Product (TRIMP). The expected outcomes of these transformations from any "pure" type of production (0, 1, 2a, 2b, or 2c) are detailed in Table 4. It must be remembered that these formalisms do not necessarily represent actual reactions but rather just "modes" of reaction and that the action of any type can lead to different profiles which depend on factors such as surface concentrations, rates, and reversibility of steps. However, qualitatively the temporal redistribution profiles and the initial distribution plots developed for each type of production must have the same individual features.

It must also be noted that for a particular "Type of Production" the atomicity of the surface intermediates (IA_x) is unimportant and the individual features of IDIMP and the qualitative features of TRIMP will remain the same; e.g., $IA_2 + I'A_2 \rightarrow PA_2 + IA + I'A$ also represents a type 2b production and $IA_3 \rightarrow PA_2 + IA$ represents type 2c production, and both will give the corresponding IDIMP and qualitative TRIMP features. Isotopic exchange of the product

molecules (through adsorption/desorption processes) with either the final intermediates or with different sites on the surface must also be allowed for. In these cases the situation becomes more complex and these will not be considered further here (see (34)). However, for many experimental cases regarding molecules such as N_2 and N_2O, these exchange reactions are not important.

In terms of the Types of Production we can also say that the overall rate of production of the two-atom molecule (PA_2) equals the sum of the individual rates of the five types of production (in a normalised form at a value of 1),

$$\chi_0 + \chi_1 + \chi_{2a} + \chi_{2b} + \chi_{2c} = 1 \qquad [9]$$

where χ_k represents the contribution of type k ($k = 0$, 1, 2a, 2b, 2c), with a rate R_k, in the overall production (with a rate R_Σ), and therefore $\chi_k = R_k/R_\Sigma$. The strict method of calculating χ_k on the basis of isotopic kinetic equations will be presented elsewhere (34). A second, simpler, but less accurate method based on IDIMP will be discussed below.

a. Initial Distribution of Isotopic Molecules of Product (IDIMP)

If we consider the overall production of an isotopic product molecule containing two "labellable" atoms following the $RA + ( ) \rightarrow {}^*RA + ( )$ switch within the SSITKA, there are normalised connections for the Initial Distribution of the Isotopic Molecules of Product; e.g.,

$$x_0^0 + x_1^0 + x_2^0 = 1 \qquad [10]$$

(where x_i^0 represents the initial fraction of isotopic molecules which contain i heavy atoms, e.g., $^{14}N_{2-i}{}^{15}N_i$). Overall, the production of N_2 remains constant, and therefore, the sum of the fractions of all isotopic molecules must, at all times, equal a normalised value of 1.

The initial isotopic product distribution following the $RA + ( ) \rightarrow R^*A + ( )$ switch (in our case $^{14}NO + O_2 + H_2 \rightarrow {}^{15}NO + O_2 + H_2$) is different for some of the types of production of PA_2 detailed above. Type 0 results in the initial distribution being fully doubly labelled, while type 1 production leads to fully singly labelled, and all type 2 productions (2a, 2b and 2c) lead to unlabelled product molecules in the initial isotopic distribution (see Table 4).

The initial isotopic distribution and the contributions of the different types of production can be related. If the probability (or contribution) of type of production k is χ_k and the initial isotopic distribution is represented as $\{x_0^0, x_1^0, x_2^0\}$, then it can be shown that

$$x_0^0 = \chi_{2a} + \chi_{2b} + \chi_{2c} \qquad [11]$$

$$x_1^0 = \chi_1 \qquad [12]$$

$$x_2^0 = \chi_0. \qquad [13]$$

That is to say, the initial distribution gives direct information about the contributions of various types of production to the overall production of PA_2.

These are obviously theoretical calculations, and it can be shown (34) that the imposition of an experimental switch rather than an ideal switch from RA to R^*A does change this distribution somewhat. In the specific case of the $NO + O_2 + H_2$ reaction over Pt/SiO_2 this makes any IDIMP analysis of the N_2O distribution more prone to errors as this is very rapid relative to the N_2 redistribution and thus more prone to effects of the imposed "experimental" switch. Generally then, with respect to the gaseous holdup of the system, the "shorter" the holdup the more accurate the IDIMP.

Plots of the IDIMP are constructed by taking the normalised values for all the isotopic molecules of N_2O and N_2 at a short time following the switch. Obviously for experimental reasons it is not possible to get readings directly after the switch (due to perturbations in the gas stream), and thus readings are taken ~3 s after the beginning of the switch. At this time the Ar has reached a normalised value of 1, the mixed-labelled products ($^{14}N^{15}N$ and $^{14}N^{15}NO$) are at maxima, and the product redistribution is in process. Taking the readings as these mixed species are at their maxima can most accurately compensate for the "experimental nature" of the switch (and its effects on the accuracy of the IDIMP analysis).

Figure 4 shows this analysis for the N_2 and the N_2O products formed following the $^{14}NO/O_2/H_2 \rightarrow {}^{15}NO/O_2/H_2$ switch at 70°C. The results are presented as bar charts showing the normalised production on the ordinate and the

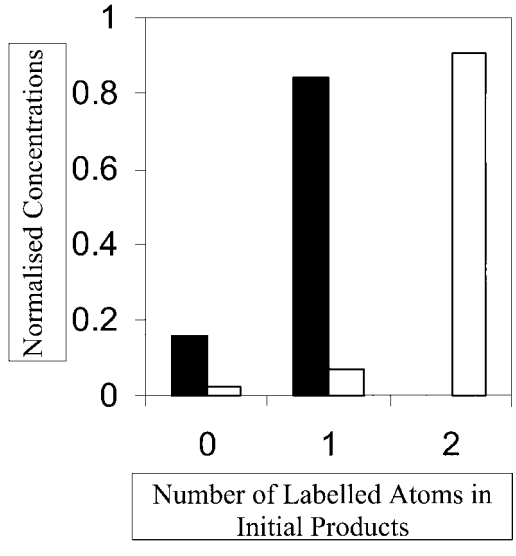

FIG. 4. IDIMP analysis of the isotopic products of the $NO/O_2/H_2 \rightarrow {}^{15}NO/O_2/H_2$ switch over 5% Pt/SiO_2 at 70°C. N_2 ■, N_2O □. (2.5% NO and H_2, 14% O_2 and He balance, to 73 cm^3 min^{-1} over 113 mg 5% Pt/SiO_2.)

number of labelled atoms on the abscissa. Most of the N_2O molecules formed at this stage are doubly labelled. From the analysis presented in Table 4, this indicates a very high level of type 0 production. However, it must be remembered that the accuracy of this is very questionable due to the rapid nature of the transient with respect to the N_2O formation.

A more interesting and informative situation is seen in the case of the N_2 IDIMP results. Here the initial distribution can be written as $\{x_0^0, x_1^0, x_2^0\} = \{0.15 \pm 0.05, 0.85 \pm 0.05, 0\}$. This can be compared to the results for the N_2 IDIMP from the NO/H_2 reaction (11), i.e., $\{0.3 \pm 0.05, 0.7 \pm 0.05, 0\}$. It can be seen that the initial fraction of the doubly labelled product is unchanged but that the mixed-labelled species is now more prominent ($0.7 \rightarrow 0.85$) and the unlabelled species is less prominent ($0.3 \rightarrow 0.15$). In terms of the contributions of various "types of production," this indicates

$$x_0^0 = \chi_{2a} + \chi_{2b} + \chi_{2c} = 0.15 \quad [14]$$

$$x_1^0 = \chi_1 = 0.85 \quad [15]$$

$$x_2^0 = \chi_0 = 0. \quad [16]$$

where χ_n represents the contribution of type of production n ($n = 0$, 1, 2a, 2b, 2c).

This shows that a type 1 production operates here (as this produces the initial amount of $^{14}N^{15}N$) as does some type 2 (a, b, or c), as this leads to the unlabelled product. Also the contribution of the "type 1" reaction is increased relative to that of some "type 2 (a, b, c)" mechanism when this reaction ($NO/O_2/H_2$) is compared to the NO/H_2 reaction under the same conditions.

We now reintroduce (11, 34) two integral characteristics which reflect the degrees of surface intermediate (or lattice) participation in the formation of doubly labelled product molecules (PA_2) from labelled molecules (RA_n) and their connection with the above-mentioned "Initial Distribution of Isotopic Molecules of Product."

First is the Coefficient of Surface Production (C_{PR})—this is the average number of surface A atoms which participate in one act of production (desorption) of a molecule PA_2. Second is the Coefficient of Percolation (C_{PE}), which is the average number of A atoms of the reactant RA which participate in one elementary act of formation of the product molecule PA_2.

In the production of the molecule PA_2 there is the obvious relationship

$$C_{PR} + C_{PE} = 2. \quad [17]$$

With regard to the five types of production the Percolation and Surface Production Coefficients for each type of production are presented in Table 4. These are derived using IDIMP and the simple equations

$$C_{PR} = 2x_0^0 + x_1^0 \quad [18]$$

$$C_{PE} = x_1^0 + 2x_2^0. \quad [19]$$

Here the values x_0^0, x_1^0, and x_2^0 represent the initial normalised fractions of the fully unlabelled, mixed labelled, and fully labelled initial product species, respectively.

In the present case (the $NO/O_2/H_2$ reaction over 5% Pt/SiO_2 at 70°C under steady-state conditions) for N_2 the $C_{PR} = 1.15$ and the $C_{PE} = 0.85$. This simply means that every molecule of N_2 produced takes an average of 1.15 N atoms from the surface and an average of 0.85 atoms from the gas phase. This compares with values of $C_{PR} = 1.3$ and $C_{PE} = 0.7$ from the NO/H_2 reaction over the same catalysts and reflects the decreased contribution of the "type 2 (a, b or c)" process for the formation of N_2 in this reaction. It is not feasible to carry out this analysis for the N_2O production since the switch is too fast.

b. Temporal Redistribution of Isotopically Labelled Molecules of Product (TRIMP)

An important characteristic of isotopically labelled molecules with more than one labelled atom of the same element is the amount of the redistribution of the isotopic equilibrium present. This is the situation in our case regarding the product molecules (N_2 and N_2O). If these molecules are in a state of isotopic equilibrium, then when the fraction of heavy isotopes (^{15}N) in the gas phase is α, the equilibrium fraction (x_i^{eq}) of the isotopic molecules, e.g., $^{15}N_i{}^{14}N_{(2-i)}$, can be calculated using the binomial distribution (28, 31)

$$x_i^{eq} = \binom{2}{i} \alpha^i (1-\alpha)^{2-i}, \quad [20]$$

where

$$\binom{2}{i} = \frac{2!}{(2-i)!\,i!} \quad \text{for } i = 0, 1, 2. \quad [21]$$

A useful probe function for the extent of isotopic equilibrium in an flow system is the deviation (y_i) of the fraction of isotopic molecules $^{14}N_{(2-i)}{}^{15}N_i$ (x_i) from their equilibrium fraction x_i^{eq}. This function was first used by Muzykantov *et al.* (28) in the analysis of isotopic exchange of O_2 in a closed system.

$$y_i = x_i - x_i^{eq} \quad \text{for } i = 0, 1, 2. \quad [22]$$

For the $^{14}N^{15}N$ molecule, which contains one heavy atom,

$$y_1 = x_1 - 2\alpha(1-\alpha). \quad [23]$$

When the isotopic molecules $PA_{2-i}{}^*A_i$ are statistically mixed, then $y_i = 0$ for $i = 0$, 1, 2. TRIMP shows the y_i variable for the isotopic molecules of product as a function of

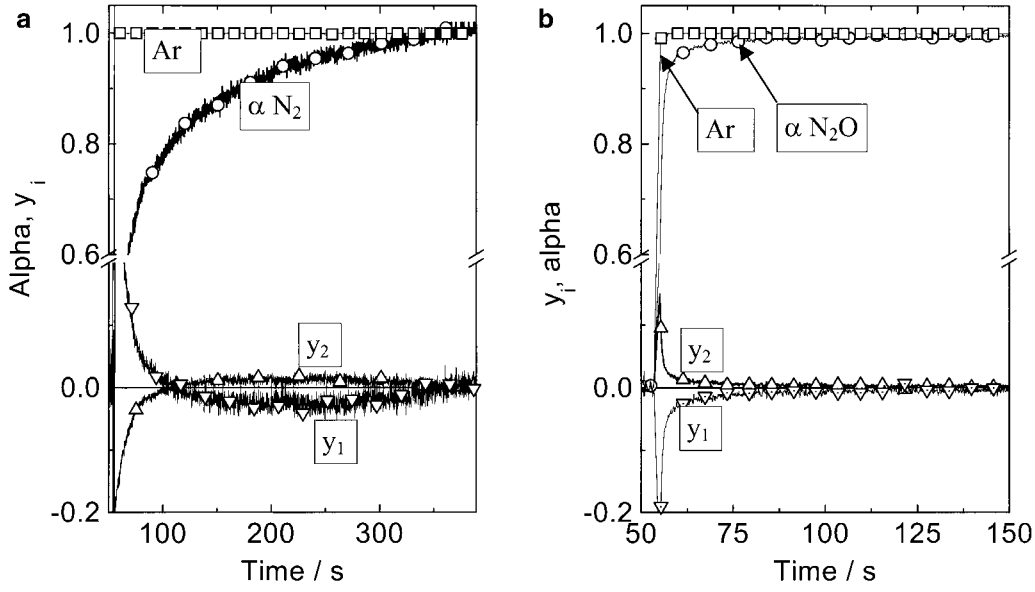

FIG. 5. TRIMP plots (in the y_i–time coordinate) for (a) $^{15}N_2$ (y_2) (△) and $^{14}N^{15}N$ (y_1) (▽) and for (b) $^{15}N_2O$ (y_2) (△) and $^{14}N^{15}NO$ (and $^{15}N^{14}NO$) (y_1) (▽) following the same experiment shown in Fig. 4. Profiles for the respective α function (○) and the inverted Ar trace (□) are also shown.

time following an isotopic step change, e.g., in our case the $^{14}NO/O_2/H_2 \rightarrow {}^{15}NO/O_2/H_2$ switches.

For a complete description of the composition of isotopic molecules, e.g., $PA_{2-i}{}^*A_i$, we only need to examine one isotopic species, i.e., (PA_2, PA^*A, or P^*A_2), in conjunction with the α profile. This is because the three deviations from equilibrium (y_0, y_1, and y_2) are related (at any time (t)) by the relationships

$$y_0(t) + y_1(t) + y_2(t) \equiv 0, \quad y_0(t) \equiv y_2(t), \quad \text{and}$$
$$y_1(t) \equiv -2^* y_0(t) (\text{or} -2^* y_2(t)). \qquad [24]$$

This indicates that the largest deviation from equilibrium will be seen for the $y_1(t)$ profile (representing the deviation from equilibrium for the $^{14}N^{15}N$ species) and that the $y_2(t)$ and $y_0(t)$ profiles (which represent the deviations for the $^{14}N^{14}N$ and the $^{15}N^{15}N$ species) will be mirror images of this profile but will be one half as intense. In this work we show both the $y_1(t)$ and the $y_2(t)$ profiles along with the α profile.

Table 4 shows how any variation in the "Type of Production" is manifested in a change in the TRIMP profiles for a plug flow reactor. For types 0 and 2a the isotopic molecules of product are always statistically mixed; i.e., $y_1 = y_2 = 0$. For types 1 and 2b there is superproduction of the mixed-labelled species for a time following the switch; i.e., $y_1 > 0 > y_2$. Conversely, for type 2c there is subproduction of the mixed-labelled species for a time following the switch; i.e., $y_1 < 0 < y_2$. These only apply in the case of "pure" types of production, and any concurrent operation of more than one type of production will lead to situations that are more complex. The operation of more than one "type" (for multiroute mechanisms) does *not* generally yield a simple profile resulting from the average of the profiles of the types involved.

The imposition of an experimental step change rather than an ideal one also causes some deviation from "true" y_i profiles in this analysis. This deviation is only seen at the beginning of the switch when the inverted Ar profile has not reached a steady value (0 in our case as ^{14}NO/Ar is removed from the stream). The TRIMP profiles for the $^{14}NO/O_2/H_2 \rightarrow {}^{15}NO/O_2/H_2$ switch are shown in Figs. 5a (N_2) and 5b (N_2O).

It can be seen that in both cases the product molecules are not in isotopic equilibrium through the course of the switch. In the case of N_2O (Fig. 5b) there is an underproduction of the mixed-labelled $^{14}N^{15}NO$ following the switch $y_1 < 0$, and this remains the situation until the $\alpha(N_2O)$ profile reaches 1. Correspondingly, there is an overproduction of the unlabelled and doubly labelled species until the $\alpha(N_2O)$ profile reaches 1. This is ascribed to the action of a "type 2c" mechanism in which the production of N_2O is through a coupled intermediate and is similar to the situation seen for N_2O production in the NO/H_2 reaction (11). This is in contrast to the IDIMP results, which indicate the action of a "type 0" mode, but it must be remembered that the IDIMP analysis is far more sensitive to the rapid nature of the switch than is the TRIMP analysis.

In the case of the TRIMP profiles for N_2 production there is an overproduction of $^{14}N^{15}N$ directly following the switch, but this turns into an underproduction ~60 s after the switch. There are two situations in which this profile can be expected. In both situations there are two routes to N_2 formation, and these operate in an "isotopically first" and an "isotopically second" type of order.

The first of these situations involves the interaction of a "type 1" impact mechanism, where gas-phase or physisorbed NO interacts with an N-containing species on the surface to form N_2 (leading to the overproduction of $^{14}N^{15}N$), and a "type 2a" mechanism, where two identical species on the surface interact to give N_2 (which in this case leads to an underproduction of $^{14}N^{15}N$). This is interesting because a pure 2a type of production yields no deviation from equilibrium but a "type 2a" in combination with a "type 1" (1 + 2a) yields this type of profile (as has been discussed in more detail previously (11)).

The second situation in which the interaction of two types of production can lead to this TRIMP profile involves a "type 1" impact mechanism (as above) in conjunction with a "type 2c" production, where the final reaction step involves a species on the surface which gives two N atoms to the N_2 molecule (coupled intermediate) (1 + 2c).

Previously (11), the y_i profiles (in the α coordinate) were used to distinguish between production via the operation of a 1 + 2a combination and that via a 1 + 2c combination. The basis of this discrimination centered around the fact that in the former case the y_1 (and y_2) profiles returned to 0 before the α value reached 1. However, in the latter case this was not what modelling predicted; i.e., y_1 remains negative until α becomes 1. In this case the data are a lot noisier than was seen in the NO/H_2 case, but it is still clear (Fig. 6) that y_1 and y_2 reach values of 0 before the α value reaches 1. Thus we can rule out a 1 + 2c mechanism in favour of a 1 + 2a one. This is a similar situation to that which was seen for the production of N_2 in the NO/H_2 reaction over Pt/SiO_2.

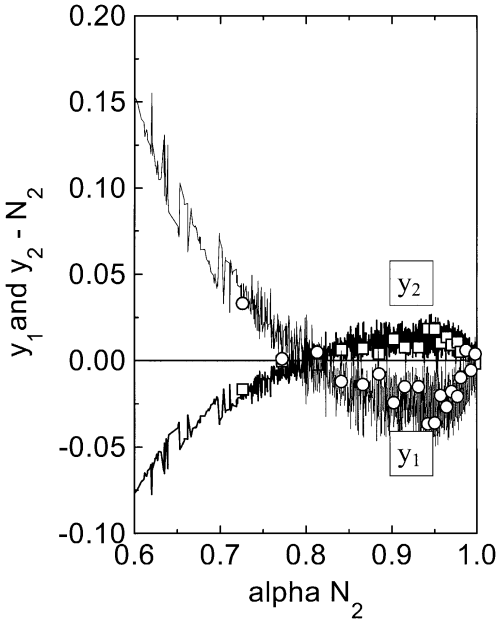

FIG. 6. The data presented in Fig. 5b presented in the y_i–α coordinate, y_1 (○) and y_2 (□).

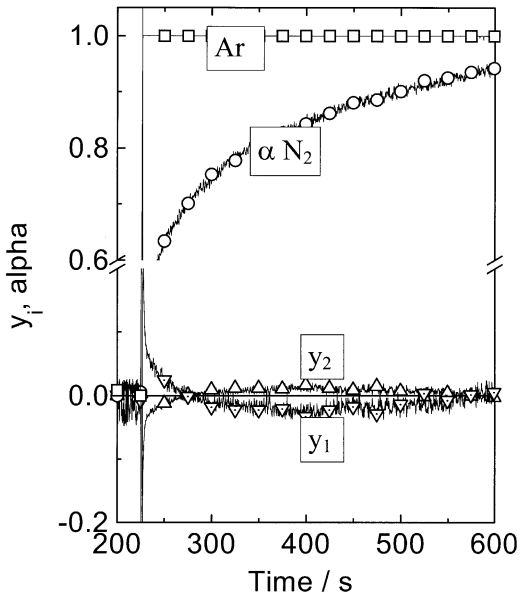

FIG. 7. TRIMP plots (in the y_i–time coordinate) for $^{15}N_2$ (y_2) (△) and $^{14}N^{15}N$ (y_1)(▽) following the $^{14}NO/H_2 \rightarrow {}^{15}NO/H_2$ switch at 70°C over 5% Pt/SiO_2 (shown for reference from (11)). Profiles for the respective α function (○) and the inverted Ar trace (□) are also shown.

Another feature of the profile which is similar to the ones taken from the $NO + H_2$ reaction is the magnitude of the underproduction of the $^{14}N^{15}N$ species. This never goes below $\sim -3\%$, indicating that the contribution of this 2a process, and thus the surface concentration of the final intermediates leading to N_2 via type 2a, is not very large (as we surmised from the IDIMP results).

One quantitative difference between this result and that seen in the NO/H_2 reaction is the larger magnitude of the overproduction of $^{14}N^{15}N$ directly following the switch, e.g., when $\alpha(N_2) = 0.6$ for both reactions following the $^{14}NO \rightarrow {}^{15}NO$ switch, $y_1 = 0.04$ in the case of the NO/H_2 reaction (Fig. 7) and $y_1 = 0.15$ in the case of the $NO/O_2/H_2$ reaction (Fig. 5a). This indicates the increased contribution of type 1 to the formation of N_2. It is also noticable that the switch is completed faster, i.e., $\alpha(N_2) = 1$, in a shorter time following the switch in the presence of O_2 (Fig. 5a) than in its absence (Fig. 7; Ref. (11)). This also qualitatively indicates the decreased contribution of the "type 2" process since it is this which is "isotopically second" in the production of N_2.

c. Semilogarithmic Plots of the $\bar{\alpha}$ Function versus Time

The semilogarithmic plots of the $\bar{\alpha}$ function versus time (11, 38) involve plotting the function $|\ln|(\bar{\alpha})||$ (where $\bar{\alpha}$ represents the $(1-\alpha)$ profile in the case of a $^{14}NO \rightarrow {}^{15}NO$ switch and the α profile in the case of the reverse $^{15}NO \rightarrow {}^{14}NO$ switch) against time. The generated profiles give information about the reaction pathways leading to products. In this case $\bar{\alpha}$ refers to $1 - \alpha$ as the switch considered is $NO + (H_2/O_2) \rightarrow {}^*NO + (H_2/O_2)$. This presentation

is derived from classical isotopic exchange analysis and is used to reflect the heterogeneity of the surface (or lattice) intermediates.

Specifically, at steady state, this presentation gives information regarding the presence of a buffer step (in which a pool of inactive intermediates could be formed, in a reversible process, from a pool of active intermediates) or the presence of a consecutive mechanism (in which one pool of intermediates goes on to form another pool of intermediates before forming a product molecule), or, for example, the presence of a mechanism in which there is only one intermediate.

In each case the semilogarithmic plot of the $\bar{\alpha}$ function versus time has a different shape. For the buffer step (first case) the curve is convex; in the consecutive mechanism (second case) it is concave; in the third case a straight line is obtained. A mechanism in which there are parallel routes leading to product and both show reversibility also yields a convex plot. Details of these different possibilities can be found in Table 5. The following shapes are expected. In the case of irreversible adsorption of reactant and desorption of product then, for a one-pool mechanism $\alpha(t)$ is a function of one exponent (24) (therefore the semilogarithmic plot of the $\bar{\alpha}$ function versus time is linear). Buffer (24) and parallel (14) pools result in $\alpha(t)$ being the sum of two exponents (the semilogarithmic plot of the $\bar{\alpha}$ function versus time is convex), and in the case of consecutive pools then $\alpha(t)$ is the difference of two exponents (24) (the semilogarithmic plot of the $\bar{\alpha}$ function versus time is concave). Combinations of these mechanisms lead to semilogarithmic plots of the $\bar{\alpha}$ function versus time that are superpositions of the former plots.

Our results are generated from modelling reversible cases of adsorption of RA and desorption of PA_2 (when $\alpha(t)$ *cannot* be represented in exponential form), and these show qualitatively similar shaped features to the situations discussed above. In the case of reversible adsorption of reactant, a situation that has heretofore been ignored, then the same transformation of the profile of the unreacted reactant (RA) can also yield information regarding the reaction network.

TABLE 5

Variations Expected in the Semilogarithmic Plots of the Function $|\ln|(\bar{\alpha})||$ against Time for Various Mechanisms for the Transformation of Reactant *R* into Product *P*

Label	Network mechanism	Shape of semilogarithmic plot (with time) $\lvert\ln(\bar{\alpha}(t))\rvert$
Direct	$R \Leftrightarrow I_1 \Leftrightarrow P$	straight line
Consecutive	$R \Leftrightarrow I_1 \Leftrightarrow I_2 \Leftrightarrow P$	concave curve
Buffer	$R \Leftrightarrow I_1 \Leftrightarrow P$ $\Updownarrow$ I_2	convex curve
Parallel	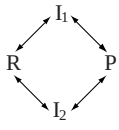	convex curve

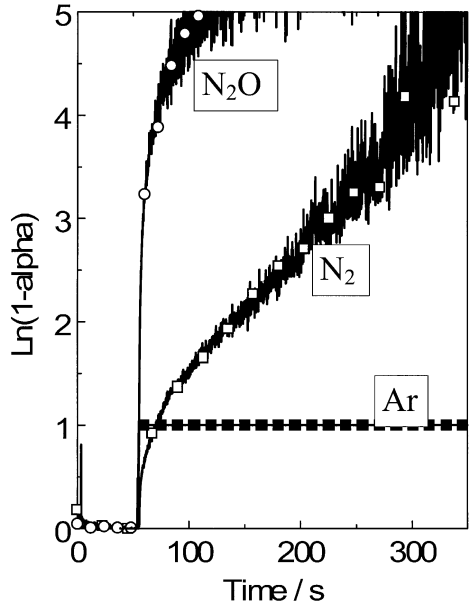

FIG. 8. Semilogarithmic plots of the function $|\ln|(\alpha)||$ against time for the product molecules N_2O and N_2, as well as an Ar profile following the $^{14}NO/H_2/O_2 \rightarrow {}^{15}NO/H_2/O_2$ switch over 5% Pt/SiO_2 at 70°C. N_2 (□), N_2O (○), inverted Ar (■).

As was the case in the IDIMP and TRIMP studies, the nature of the "gas-phase holdup" can affect the shape of these profiles. However, in this case the effect is far less severe. The relationship between the "gas-phase holdup" and the α(product) response (in the case of irreversible adsorption/desorption) has been previously derived (39).

In our case the semilogarithmic plot of the $\bar{\alpha}$ function versus time for the production of both N_2 and N_2O is shown with a standard Ar response in Fig. 8. Both of these are convex, and thus both sets of intermediates (of N_2 and N_2O) must have buffer states or possibly are formed from parallel mechanisms such as those detailed in the fourth row of Table 5. Qualitative analysis of the profiles indicates that the probability of the latter is not high, and therefore we must incorporate some buffer states within the reaction mechanism for the production of N_2 and N_2O. It must also be pointed out that these cannot be the same species for the formation of N_2 and N_2O.

It is seen that the N_2O profile is far sharper than that of the N_2. This is to be expected since the transient in N_2O is itself far quicker than that for N_2 (N_2O is the isotopically first product). A value of 4 in the semilogarithmic plot is indicative of 99% transference of the heavy (^{15}N) isotope into the product molecules.

PROPOSED MECHANISM

From this analysis, we can propose a mechanism for the conversion of the $NO/H_2/O_2$ reaction mixture to N_2/N_2O and NO_2 over Pt/SiO_2 catalysts, and there are several points which we can determine from our analysis to be correct. These are:

- the experiments show that N_2O is "isotopically first" and the proposed mechanism must be consistent with this;
- from the TRIMP analysis we know that there are two routes to N_2 formation; furthermore, we can describe the features of the "final surface steps" involved in each of these routes ((a) for example an interaction between a weakly adsorbed species which is in rapid equilibrium with the gas-phase NO and a chemisorbed species, each of which donates one single N atom to the final N_2 product; (b) the interaction of two equivalent chemisorbed species on the surface, each donating one single N atom to the N_2 product);
- the relative contributions of each of these routes to N_2 formation;
- the route to NO_2 formation is through both gas-phase and surface reactions;
- the route to N_2O formation is through a final step involving a coupled intermediate (which donates two N atoms to the final N_2 product) on the surface;
- N_2O formation requires the presence of a species in reversible equilibrium with the gaseous NO;
- there are buffer states on the surface for intermediates in the formation of N_2 and N_2O and these cannot be the same for both products.

Using this information we can consider the possible chemical nature of the various intermediates and the types of paths the intermediates follow to the final products. It must be remembered that this information gives a formalism to the intermediates (we know how many N atoms yielded per intermediate to product), the reaction steps (we know the nature of the final interactions), and the network mechanism (we know that there is a buffer state), but it cannot shed light on the absolute chemical nature of the intermediates or their reaction. For this information a more detailed study involving *in situ* spectroscopic techniques would be needed.

Scheme 1 shows a plausible reaction network in which, for convenience, we have allocated precise descriptions to the various species. Again, we stress that the actual chemical nature of the proposed surface species is speculative, but those chosen seem intuitively reasonable. For example, we refer to an NO_{preads} species. We know that this species leads to N_2 and N_2O production, that it is weakly bound to the surface, that it donates one N atom in N_2 formation, and that it is in rapid equilibrium with the gas phase. However, we do not know its exact chemical form.

The mechanism of the reaction has similarities to that previously proposed for the NO/H_2 reaction in the absence of O_2 although there are important differences of detail. The main feature is that N_2 and N_2O are formed in parallel through a weakly adsorbed surface species which is in rapid equilibrium with the gaseous NO (represented as NO_{preads}).

With respect to N_2O formation we can say that the reaction is very fast, requires a weakly adsorbed species, has a

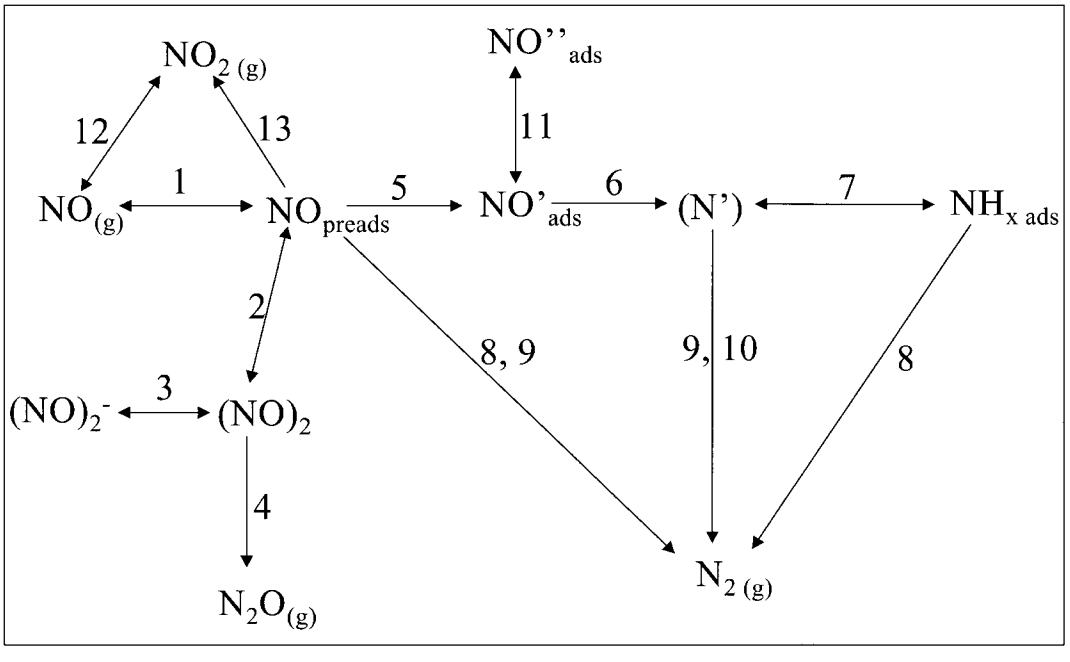

SCHEME 1. Network of NO conversion into N_2O and N_2 over 5% Pt/SiO_2 in the $NO/O_2/H_2$ reaction as derived from SSITK Analysis.

surface intermediate which contains two N atoms, and has a buffer step.

The mechanism presented in Scheme 1 shows the adsorption of NO to form a preadsorbed state (step 1). This then dimerises (step 2) to form an $(NO)_2$-type species that can be stabilised by the addition of an electron $(NO)_2^-$ (step 3). The dimer can also decompose to form N_2O (step 4). We know that the final intermediate before the formation of N_2O on the surface gives two N atoms to the N_2O molecule, so the proposition of a dimeric $(NO)_2$ species is not unreasonable. We also know that there is a buffer state on the route to N_2O formation. We have represented this as the dimeric species stabilised by the addition of an electron $(NO)_2^-$. This intermediate has been previously proposed as an intermediate in N_2O formation from NO over Pt-based catalysts (40).

In the formation of N_2 we must account for two routes. Again, all we can definitely say about the first route is that there is an interaction between a gaseous (or physisorbed) NO molecule with a surface species containing one N atom and that this interaction leads to ~85% of the N_2 formed from the reaction. This can be envisaged as step 8, where the physisorbed NO molecule reacts with a reduced N-containing species (NH_x) on the surface. The reduced N-containing species must be formed from the chemisorption of the preadsorbed NO molecule (step 5) and the reduction of this species (steps 6 and 7). Another possibility for this "type" of production can be chemically represented as the interaction of the physisorbed NO with another "N" species, e.g., formed via the decomposition of the NO_{ads} species in Step 6, as the type 1 route, in an $NO_{preads} + N_{ads} \rightarrow N_2 + O_{ads}$ reaction. This form of N_2 production is represented as step 9 in the scheme.

The second mechanism of N_2 formation (accounting for ~15% of the N_2 formed) is via the interaction of two identical surface intermediates, both of which give one N atom to the N_2 product. This is represented in the scheme as step 10 and can be thought of as $N_{ads} + N_{ads} \rightarrow N_2$. Again, we cannot exclude other interactions leading to this "type" of production, e.g., $NO_{ads} + NO_{ads} \rightarrow N_2$ or $NHx_{ads} + NHx_{ads} \rightarrow N_2$. All we can definitely state is that there is a route of formation to N_2 which involves the interaction of two equivalent surface species. We also know that there is a buffer state present somewhere in the reaction scheme, and this is represented as NO″—formed in step 11.

The formation of NO_2 is also considered in the scheme as coming from gas-phase NO (step 12) or the interaction of the chemisorbed NO molecule with O_{ads} on the surface (step 13).

The presence of different forms of chemisorbed NO and atomic N species on Pt has been reported previously using an SERS technique (41). Spectroscopic evidence for the presence of $(NO)_2$ intermediates has been presented for NO adsorption on Pt (42). NHx species have also been reported on Pt by using a HREELS technique (43). Therefore, although in our mechanistic analysis we cannot identify specific surface intermediates, all those which are postulated in Scheme 1 are known to exist under different conditions on Pt catalysts. However, these experimental observations are obtained under different reaction conditions, and our analysis simply gives formal identities to the individual species.

CONCLUSIONS

A mechanism has been proposed for the $NO/O_2/H_2$ reaction over Pt/SiO_2. The main products (N_2 and N_2O) are formed in a parallel mechanism through a preadsorbed NO intermediate. This involves the formation of N_2O as a very rapid process which moves through an intermediate containing two N atoms on the surface. There are two routes for the formation of N_2. One is through an impact mechanism (where physisorbed NO interacts with a reduced N-containing species on the surface). This is a type 1 production and leads to ~85% of the N_2 formed. The second route involves two identical species on the surface, which combine to form N_2 (both species giving one N atom to the final product). This is a type 2a production and leads to ~15% of the N_2 formation. The contribution of the latter route is decreased relative to its contribution in the NO/H_2 reaction, and correspondingly the contribution of the former (impact) route is increased. Every N_2 molecule formed takes an average of 1.15 N atoms from the surface and an average of 0.85 N atoms from gaseous NO.

We conclude that the effect of the excess of O_2 on the NO/H_2 reaction is to remove the higher temperature deNOx activity, suppress NH_3 formation, form NO_2, and decrease the *overall* amount of N_2 and N_2O formed. These effects can be thought of as being due to competitive adsorption between the NO and O_2 (or between the H_2 and the O_2). The overall mechanisms of N_2 and N_2O formation are unchanged although the relative contributions of different types of N_2 production are different.

ACKNOWLEDGMENTS

We are grateful to the EPSRC for supporting this research through contract GR/K70403. A.A.S. thanks NATO and The Royal Society for providing a Fellowship (NATO/96A).

REFERENCES

1. Taylor, K. C., *Catal. Rev. Sci. Eng.* **35**(4), 457 (1993). [And refs. therein]
2. *Catal. Today* **26** (1995). [R. Burch, Ed.]
3. Iwamoto, M., and Mizuno, N., *J. Automobile Eng.* **207**, 23 (1993).
4. Ansell, G. P., Golunski, S. E., Hayes, J. W., Burch, R., and Millington, P. J., *Stud. Surf. Sci. Catal.* **96**, 577 (1995).
5. Burch, R., and Watling, T. C., *Catal. Lett.* **43**(1–2), 19 (1997).
6. Captain, D. K., Robberts, K. L., and Amaridis, M. D., *Catal. Today* **42**, 93 (1998).
7. Sasaki, M., Hamada, H., Kintaichi, Y., Ito, Y., and Tabata, M., *Catal. Lett.* **15**, 297 (1992).

8. Burch, R., Fornasiero, P., and Watling, T. C., *J. Catal.* **176**, 204 (1998).
9. *Catal. Today* **22**, (1994). [M. Iwamoto, Ed.]
10. Burch, R., and Coleman, M. D., *Appl. Catal. B Environ.*, in press.
11. Shestov, A. A., Burch, R., and Sullivan, J. A., *J. Catal.* **186**, 362 (1999). [NO/H_2, Part 2]
12. Yokota, K., Fukui, M., and Tanaka, T., *Appl. Surf. Sci.* **121–122**, 273 (1997).
13. Frank, B., Emig, G., and Renken, A., *Appl. Catal. B Environ.* **19**, 45 (1998).
14. Shannon, S. L., and Goodwin, J. G., *Chem Rev.* **95**, 677 (1995).
15. Mirodatos, C., *Catal. Today* **9**, 83 (1991).
16. Happel, J., *Chem. Eng. Sci.* **33**, 1567 (1978).
17. Bennett, C. O., *in* "Catalysis Under Transient Conditions" (A. T. Bell and L. L. Hegedus, Eds.), ACS Symposium Series, Vol. 178, p. 1. Am. Chem. Soc., Washington DC, 1982.
18. Biloen, P., *J. Mol. Catal.* **21**, 17 (1982).
19. Hanssen, K. F., Blekkan, E. A., Schanke, D., and Holmen, A., *Stud. Surf. Sci. Catal.* **109**, 193 (1997).
20. Kumthekar, M. W., and Ozkan, U. S., *J. Catal.* **171**(1), 54 (1997).
21. Burch, R., Shestov, A. A., and Sullivan, J. A., *J. Catal.* **182**(2), 497 (1999).
22. Godfrey, K., "Compartmental Models and Their Application." Academic Press, London, 1983.
23. Happel, J., Walter, E., and Lecourtier, Y., *I&EC Fundam.* **25**, 704 (1986).
24. Happel, J., Walter, E., and Lecourtier, Y., *J. Catal.* **123**, 12 (1990).
25. Nibbelke, R. H., Scheerova, J., de Croon, M. H. J. M., and Marin, G. B., *J. Catal.* **156**, 106 (1995).
26. Kemball, C., *Adv. Catal.* **11**, 223 (1959).
27. Klier, K., Novakova, J., and Jiru, P., *J. Catal.* **2**, 479 (1963).
28. Muzykantov, V. S., Popovskii, V. V., and Boreskov, G. K., *Kinet. Catal.* **5**(N4), 624 (1964).
29. Boreskov, G. K., and Muzykantov, V. S., *Ann. N.Y. Acad. Sci.* **213**, 137 (1973).
30. Muzykantov, V. S., *React. Kin. Catal. Lett.* **33**, 937 (1987).
31. Boreskov, G. K., *in* "Catalysis, Science and Technology," Vol. 3, p. 39. Springer-Verlag, New York, 1982.
32. Winter, E. R. S., *J. Chem. Soc. (A)*, 2889 (1968).
33. Ozaki, A., *in* "Isotopic Studies of Heterogeneous Catalysts." Academic Press, New Work, 1977.
34. Shestov, A. A., Burch, R., and Sullivan, J. A., to be submitted.
35. Burch, R., Shestov, A. A., and Sullivan, J. A., unpublished work.
36. Mirodatos, C., *J. Phys. Chem.* **90**, 681 (1986).
37. Mirodatos, C., Dalmon, J. A., and Martin, G. A., *J. Catal.* **105**, 405 (1987).
38. Shestov, A. A., Burch, R., and Sullivan, J. A., in preparation.
39. Shannon, S. L., and Goodwin, J. G., *Appl. Catal. A Gen.* **151**, 3 (1997).
40. Acke, F., Ph.D. thesis, University of Göteborg, Sweden, 1998.
41. Williams, C. T., Toila, A. A., Chan, H. Y. H., Yakoudis, C. G., and Weaver, M. J., *J. Catal.* **163**, 63 (1996).
42. Yoshinobu, J., and Kawai, M., *Chem. Letts.*, 605 (1995).
43. Zemlyanov, D. Y., Smirinov, M. Y., Gorodetskii, V. V., and Block, J. H., *Sur. Sci.* **329**, 61 (1995).